

2.0 Atomic modelling relevant to neutral beam driven diagnostic

2.1 Introduction

To fully exploit the diagnostic potential of injecting neutral atomic beams into tokamak plasmas, a detailed knowledge of the attenuation and the excited state population structure of the neutral beam atoms is required. To obtain such information requires quite elaborate statistical models which include detailed descriptions of the atomic processes which contribute to exciting and ionising the penetrating beams. The pathways through the complexity depends on the conditions of the plasma, the ranking of atomic and plasma lifetimes and the actual beam atoms themselves.

In this chapter we discuss the broad assumptions which are employed to enable us to model the attenuation and excited state population structure of neutral deuterium and helium beam atoms. We then summarise the particular primary and secondary atomic processes which are involved for each beam species. We illustrate in detail the behaviour of each process as a function of energy since this allows one to quantitatively assess the varying and relative influence of each atomic process. Finally, we explain the choice of statistical models which we employ and give a historical review of previous modelling approaches by others.

2.2 Physical conditions and separation of time scales

2.2.1 Thermodynamic equilibrium

For a plasma which has reached thermodynamic equilibrium, the distribution of the plasma particles on an atomic level can be described using equilibrium statistical mechanics. The radiation field in such a plasma is free of any spectral lines and is that of a blackbody. The radiation field is Plankian with an energy density,

$$U(\nu) = \frac{8\pi h \nu^3 d\nu / c^3}{\exp(h\nu / k_B T_r) - 1} \quad 2.1$$

where k_B is boltzmann's constant, ν is the frequency of the photons and T_r is the temperature of the radiation field which is equal to both the electron and ion temperature.

The velocity distribution and the excited state population structure of the plasma constituents can be described by Maxwell-Boltzmann statistics. For a particle of mass m and temperature T the speed distribution is Maxwellian,

$$f(v) = 4\pi v^2 \left(\frac{m}{2\pi k_B T} \right)^{\frac{3}{2}} \exp\left(-\frac{mv^2}{2k_B T} \right) \quad 2.2$$

where v is the particle velocity.

The excited state population distribution of a single atom or ion contained in the plasma is given by Boltzmann's equation which relates the population of two levels, N_i and N_j , their statistical weights and their excitation energies as,

$$\frac{N_i}{N_j} = \frac{w_i}{w_j} \exp\left(-\frac{(E_i - E_j)}{k_B T} \right) \quad 2.3$$

When the population distribution of more than one ionisation stage of a particular species are compared, we can extend Boltzmann's equation to describe the excited state population of one ionisation stage relative to the ground state of the next ionisation stage. This is called the Saha-Boltzmann equation which is given as,

$$N_i = n_e n_+ 8 \left(\frac{\pi a_0^2 I_H}{k T_e} \right)^{\frac{3}{2}} \frac{w_i}{2w_+} \exp\left(\frac{I_i}{k T} \right) \quad 2.4$$

where N_i and w_i are respectively the population and statistical weight of the level i . The quantity n_+ is the population of the ground state of the next ionisation stage, w_+ is the corresponding statistical weight and n_e is the free electron number density.

There is yet another useful property associated with plasmas which are in thermodynamic equilibrium. That is the principle of detailed balance. The distribution of energy amongst the electrons and ions has reached equilibrium at a particular temperature, therefore the rate at which atomic processes contribute to

populating or depopulating excited levels of ions or atoms contained in the plasma will be balanced by the rate of the corresponding reverse processes. In such circumstances we describe the forward atomic processes to be in detailed balance with the reverse processes. For example, spontaneous and stimulated emission would be in detailed balance with photo-excitation. This principle can be used to arrive at relationships which connect the coefficients used to describe the rate at which the forward and reverse reaction of a particular atomic process occurs. If we consider electron impact excitation for which the corresponding reverse reaction is electron impact de-excitation, it can be shown using equation 2.3 that the rate coefficients for the forward ($q_{i \rightarrow j}$) and the reverse ($q_{j \rightarrow i}$) reaction satisfies the relationship,

$$q_{i \rightarrow j} = q_{j \rightarrow i} \frac{w_i}{w_j} \exp\left(-\frac{(E_i - E_j)}{k_B T_e}\right) \quad 2.5$$

where T_e is the electron temperature. Therefore the rate coefficient for electron impact de-excitation can be obtained from the rate coefficient for electron impact excitation and vice versa.

2.2.2 Local thermodynamic equilibrium

Tokamak plasmas however are far from thermodynamic equilibrium. This is primarily due to the fact that radiation can easily escape from the plasma. Under normal operating conditions tokamak plasmas are optically thin to their own radiation. Due to the magnetically confined particles though the plasma does approach conditions which are near to thermodynamic equilibrium. Elastic collisions between electrons and between protons and between electrons and protons are efficient to establish Maxwellian velocity distributions. Excited levels of atoms and ions in the plasma which are populated and depopulated by electron and proton collisions approach values that would have been obtained as if the plasma was in thermodynamic equilibrium. This condition is called local thermodynamic equilibrium, LTE. For excited levels which are in LTE, Maxwell-Boltzmann statistics are valid.

The formation of LTE conditions in a plasma is governed by the rate at which the plasma constituents take up Maxwellian distributions. For free particle distributions as discussed by Spitzer[28], this is characterised by so-called slowing down times. The slowing down time describes the rate at which the kinetic energy distribution between two elastic collision partners approaches that of a Maxwellian. In the tokamak plasma we are concerned with electron-electron, proton-proton and electron-proton relaxation. The electron-proton slowing down time is usually referred to as the equilibration time. The slowing down time associated with electron-electron collisions (τ_{e-e}) is given by Spitzer (see page 133),

$$\tau_{e-e} = 0.266 \frac{T_e^{3/2}}{n_e \ln \Lambda} \quad 2.6$$

where T_e and n_e are respectively in units of $^{\circ}\text{K}$ and cm^{-3} . The quantity $\ln \Lambda$ is the Coulomb logarithm for which tabulated values are also given by Spitzer. Similar formulae give the slowing down time for proton-proton collisions (τ_{p-p}) and the equilibration time between electrons and protons (τ_{eq}) and these are related by,

$$\tau_{p-p} \approx \left(\frac{m_p}{m_e} \right)^{1/2} \tau_{e-e} \quad \tau_{p-p} \approx 43 \tau_{e-e} \quad 2.7$$

$$\tau_{eq} \approx \frac{m_p}{m_e} \tau_{e-e} \quad \tau_{eq} \approx 1836 \tau_{e-e} \quad 2.8$$

In the context of the present work it is instructive to compare the slowing down and equilibration times to the energy confinement time of the JET tokamak plasma. This will enable us to assess if the free particle Maxwellians are achieved in a tokamak plasma and the degree to which Maxwell-Boltzmann statistics can be applied to highly excited ion populations. In table 2.1 we show the slowing down and equilibration times for a plasma with a temperature of 2.0×10^3 eV as a function of electron density.

$N_e (cm^{-3})$	1.0×10^{13}	3.0×10^{13}	5.0×10^{13}	7.0×10^{13}	1.0×10^{14}
$\tau_{e-e} (s)$	$\sim 2.1 \times 10^{-4}$	$\sim 7.0 \times 10^{-5}$	$\sim 4.2 \times 10^{-5}$	$\sim 3.0 \times 10^{-5}$	$\sim 2.1 \times 10^{-5}$
$\tau_{p-p} (s)$	$\sim 9.0 \times 10^{-3}$	$\sim 3.0 \times 10^{-3}$	$\sim 1.8 \times 10^{-3}$	$\sim 1.2 \times 10^{-3}$	$\sim 9.0 \times 10^{-4}$
$\tau_{e-p} (s)$	~ 0.3	~ 0.1	~ 0.07	~ 0.05	~ 0.03

Table 2.1 Slowing down and equilibration times. The temperature was 2.0×10^3 eV and the Coulomb logarithm was taken to be approximately 14.

The confinement time of the JET tokamak plasma is approximately 1.0 second, therefore from table 2.1 it can be seen that the formation of free particle Maxwellians can easily be achieved. It should be noted though that excited levels of ions and atoms which are primarily populated and depopulated by radiative processes do not satisfy the criteria for LTE. This occurs for low lying excited levels where collisional redistribution is less effective. This condition is described as non local thermodynamic equilibrium, non-LTE. In non-LTE environments Maxwell-Boltzmann statistics can not be used to describe the excited state population structure of plasma ions and atoms and an alternative method is sought.

2.2.3 Statistical balance equations

A general approach used to obtain the population of non-LTE and LTE levels is by solution of the statistical balance equations. The statistical balance equations represent the rate at which the excited levels of an atom or an ion are populated and depopulated. In the present work, where we are interested in modelling the excited population structure of neutral beam atoms, the statistical balance equations are,

$$\frac{dN_i}{dt} + v_b \frac{dN_i}{dx} = \left(\text{Populating} \rightarrow N_i \right) - \left(\text{Depopulating} \leftarrow N_i \right) \quad 2.9$$

for $i=1, 2, 3...$

where v_b is the beam velocity and dx is along the beam path. The terms in the brackets on the right hand side represent the rate at which the atomic processes contribute to populating and depopulating each of the excited levels of the beam

atoms, whilst the terms on the left hand side include a spatial and time dependent derivative. The spatial derivative represents the rate at which the populations change due to alterations in the local environment as the beam atoms continue into the plasma. The time derivative accounts for a change in the population due to a variation in the source of the beam atoms. The neutral beams which are of interest in this thesis however are considered to be steady state sources and the time derivative of equation 2.9 can be set to zero i.e. $dN_i/dt = 0$. The solution of the above equations yield the population density of each level, N_i , and as discussed later, further manipulation of the equations enables one to describe the attenuation of the beam atoms.

2.2.4 Ranking of atomic lifetimes

The method of solving the statistical balance equations is now the point of interest. To determine the most convenient method of solution one has to compare the time scales on which the local plasma conditions change relative to the lifetimes associated with the excited levels of the neutral beam atoms. The local plasma conditions include the electron and ion density as well as their associated temperatures. If the atomic lifetimes are short in comparison to the time scales on which the local conditions change, the excited states of the beam neutrals can relax and achieve a steady-state equilibrium population. In such circumstances we can reduce the statistical balance equations to a simple system of linear equations i.e. $v_b dN_i/dx = 0$. We call this the quasi-static equilibrium solution. If however the local conditions change more rapidly which prevents the excited states to relax, a spatially dependent solution of the statistical balance equations is necessary.

The atomic lifetimes associated with the excited levels of an atom can vary enormously. However it is possible to separate the excited levels into three distinct categories according to their lifetime[29]. These are autoionising, ordinary and metastable levels. The lifetime of these levels respectively satisfy the inequality,

$$\tau_a \ll \tau_o \ll \tau_m \tag{2.10}$$

where τ_a is $\sim 10^{-12}$ s, τ_o is equal to the reciprocal of the associated transition probability and $\tau_m \sim 10/z_0^4$. To quantitatively assess the time scales on which the local conditions of the plasma change involves evaluating scaled lengths for both the electron and ion density and their respective temperatures[30]. The scaled lengths represent the spatial distance over which the beam atoms can travel before the former and latter parameters begin to change substantially. As an example the scaled length for the electron density is defined as,

$$\ell_{n_e} = \left[\frac{1}{n_e} \frac{dn_e}{dx} \right]^{-1} \quad 2.11$$

It is more convenient though to convert the scaled length into an apparent lifetime using the relation,

$$\tau_{n_e} = \frac{\ell_{n_e}}{v_b} \quad 2.12$$

The lifetime gives the time scale on which the electron density changes and can be used to compare with the atomic lifetime of the beam atoms. The time scales on which the remaining plasma parameters change are also obtained in a similar manner. In the present work though, to a good approximation, the time scales on which the local plasma conditions alter (τ_d) is comparable to the lifetime of the metastable levels. Therefore we can then extend the ranking of the lifetimes,

$$\tau_a \ll \tau_o \ll \tau_m \approx \tau_d \quad 2.13$$

In the case of modelling the excited population structure of neutral deuterium beam atoms, from the ranking of atomic lifetimes the excited states will reach an equilibrium population. To obtain the excited state population structure the statistical balance equations, excluding the ground state, can be reduced to a system of linear equations i.e. $\sum v_b dN_i/dx = 0$, see section 3.2.

Modelling the excited state population structure of a neutral helium beam is some what different. The presence of two excited metastable levels ($\text{He}(2s \ ^1S)$, $\text{He}(2s \ ^3S)$) complicates the modelling. In any case the excited states, excluding the

two metastable levels, will approach an equilibrium population. The statistical balance equations can be reduced to a system of linear equations with the exception of the ground and the two metastable levels i.e. $\sum v_b dN_i/dx = 0$, see section 3.3. It should be noted that it is also important to be able to calculate the population of the non-equilibrium metastable levels. This can be achieved via a spatially dependent solution of the statistical balance equations, see chapter 6.0.

2.3 Atomic processes associated with a neutral deuterium beam

The penetration of a neutral deuterium beam into a plasma is governed by the behaviour of the primary and secondary atomic processes which contribute to stripping the electrons from the neutral beam atoms. The primary atomic processes we consider first are for a pure D^+ plasma and are those which directly deplete the ground state, namely direct charge exchange as well as electron and ion impact ionisation. In figure 2.1 we show the fundamental cross sections for each process.

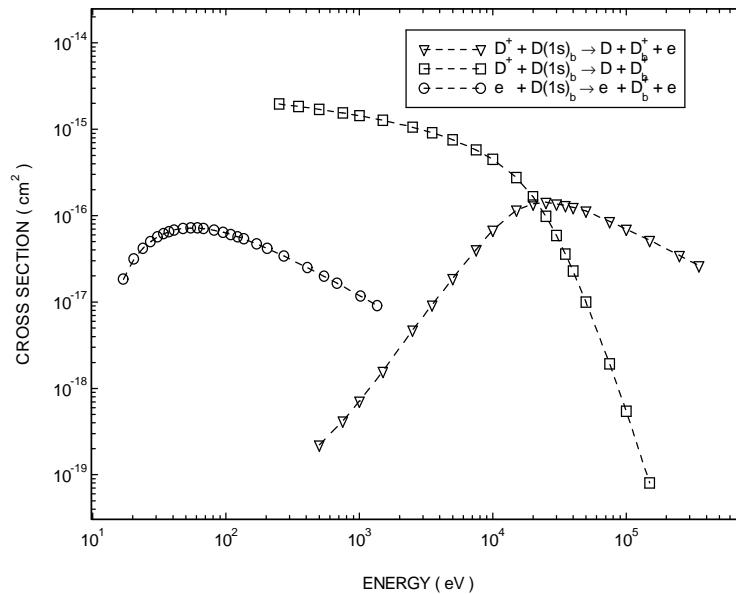


Figure 2.1 Cross sections for the direct atomic process associated with deuterium beam atoms.

As can be observed the contribution from each atomic process is determined by the relative collision energy. Charge exchange dominates until around 20 keV where the influence of ion impact ionisation becomes important. We emphasise that figure 2.1 shows the fundamental cross sections and not the rate coefficients, therefore the

contribution due to electrons appears to be very small. It should be noted that the electrons are moving with a velocity which is approximately 60 times faster than the D^+ ions and the resultant rate coefficient will be significant. Nevertheless charge exchange marginally remains the dominant process at the low energies.

The secondary atomic processes, which influence the ionisation of a penetrating deuterium beam, can be subdivided into two categories. The first category concerns bound-bound processes which excite the beam atoms and then contribute to the collisional and radiative redistribution amongst their excited states. The second category are the bound-free collisional processes which deplete the excited state populations. In the present context however we restrict ourselves to discussing the behaviour of the bound-bound and bound-free collisional processes, since under optically thin plasma conditions the only significant radiative process is that of spontaneous emission.

Collisional excitation and redistribution amongst the excited states are driven by electron and ion impact from the ground and neighbouring excited states. In the plasma, these processes are also accompanied by their corresponding reverse reactions, that is electron and ion impact de-excitation. In figure 2.2 we contrast the behaviour of the excitation cross sections for collisions with ions (D^+) and electrons. As can be observed, electron impact excitation is dominant at the lower energies. As the energy is increased, the contribution due to electron impact excitation becomes negligible as ion impact excitation becomes important.

The dominant bound-free processes responsible for ionising the excited state populations include ion impact ionisation and charge exchange. In figure 2.3 we contrast the behaviour of each process as a function of energy for different principal quantum shells. Also shown is the behaviour of electron impact ionisation from the $n=2$ and $n=3$ shell.

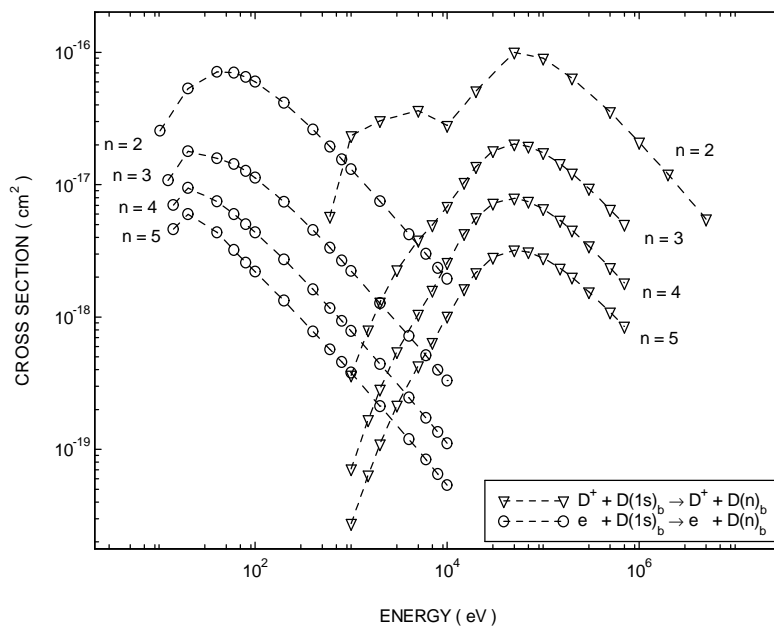


Figure 2.2 Cross sections for electron and ion impact excitation from the ground state to the $n = 2$, 3, 4 and $n=5$ shell.

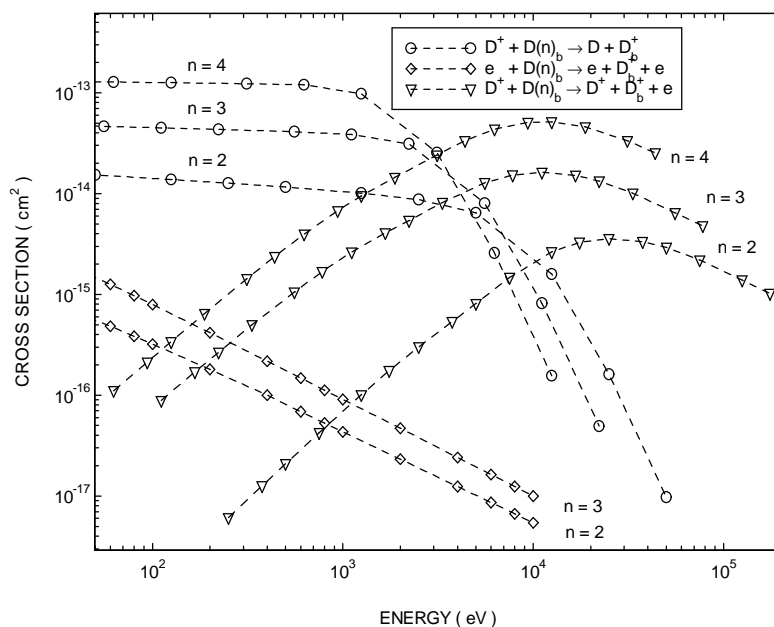


Figure 2.3 Impact ionisation and charge exchange cross sections associated with the $n=2$, 3 and $n=4$ shell.

As shown in figure 2.3, the contribution due to electron impact ionisation appears to be small due to the presence of charge exchange which is dominant up to 3.0 keV,

see earlier. We note the magnitude of the charge exchange and ion impact ionisation cross sections which increase with the principal quantum number (c.f. figure 2.1).

In tokamak plasmas the atomic processes associated with impurity ions should also be given some consideration, due to their unavoidable presence they can also contribute to stripping the electron from the neutral beam atoms. In figure 2.4 we show the cross sections for direct charge exchange and ion impact ionisation of the beam atoms due to collisions with a select range of fully stripped ions which are common plasma impurities.

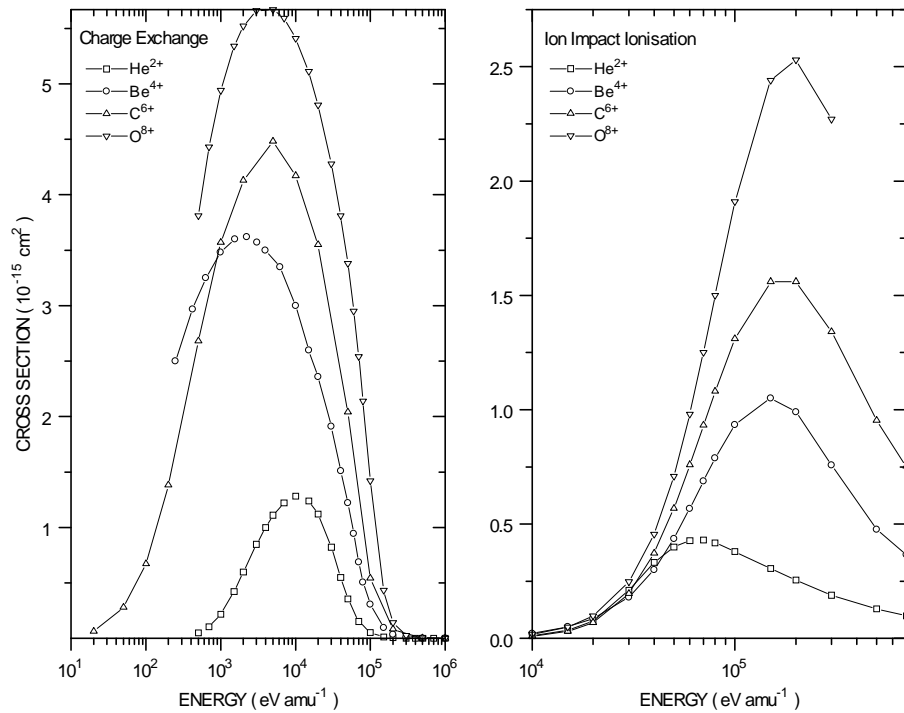


Figure 2.4 Cross sections for direct charge exchange and ion impact ionisation of the deuterium beam atoms for a selected range of fully stripped plasma impurity ions. The figure to the left exhibits the charge exchange cross sections while the figure to the right shows the behaviour of ion impact ionisation cross sections.

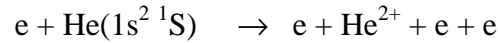
It can be observed from both figures, that the magnitude of the cross sections which describe each process increase with nuclear charge. Similar observations can be made for the remaining atomic processes associated with each of the impurity ions. These include ion impact excitation as well as charge exchange and ion impact ionisation from the excited states of the beam neutrals. The concentration of each impurity ion

in a tokamak plasma is small ($< 5\%$), however due to their large cross sections their influence on stripping the electrons from the beam atoms is comparable to that of the D^+ ions which is the main constituents of the plasma ($> 90\%$).

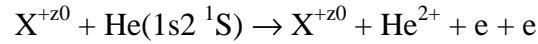
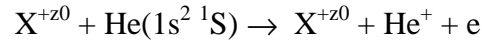
2.4 Atomic processes associated with a neutral helium beam

The penetration of a neutral helium beam into a tokamak plasma can similarly be characterised by the primary and secondary atomic processes which contribute to stripping the electrons from the neutral beam atoms. Due to the presence of two bound electrons associated with the beam atoms, both of which may be active, the variety and complexity of the primary and secondary processes increases substantially over that for a deuterium beam. The main processes are as follows,

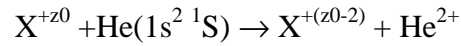
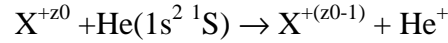
- (i) Single and double electron impact ionisation



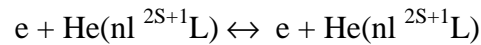
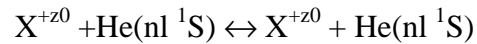
- (ii) Single and double ion impact ionisation



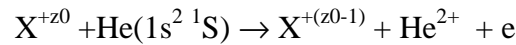
- (iii) Single and double charge exchange



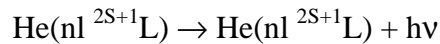
- (iv) Ion and electron impact excitation / de-excitation



- (v) Transfer double ionisation



- (vi) Spontaneous emission



The primary atomic processes which are responsible for directly stripping the electrons from the neutral helium beam atoms include single and double impact

ionisation, single and double charge exchange as well as single transfer ionisation. In figure 2.5 we show the cross sections which describe the behaviour of each of these processes.

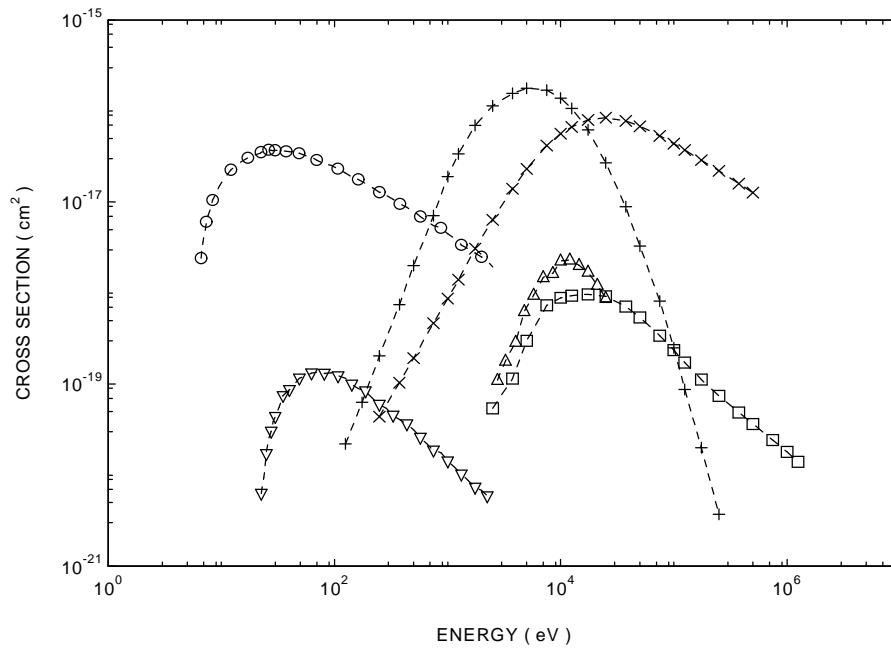


Figure 2.5 Cross sections for the primary atomic processes which contribute to stripping the electrons from the He($1s^2 \ ^1S$) ground state of the beam atoms. ○ : Single electron impact ionisation, ∇ : Double electron impact ionisation, + : Single charge exchange, × : Single ion impact ionisation, Δ : Transfer double ionisation, : Double ion impact ionisation .

As can be observed the role of single electron impact ionisation dominates at the lower energies. At ~ 750 eV single charge exchange becomes important and a competition between single ion impact ionisation commences. The competition continues until around ~ 17.5 keV where single ion impact ionisation becomes substantial.

In the same manner as discussed in section 2.3 for a deuterium beam, the secondary atomic processes which contribute to exciting and ionising a penetrating helium beam can be categorised into two sections. The first category concerns bound-bound processes whilst the second includes bound-free. We confine ourselves here to describing only the behaviour of bound-bound and bound-free collisional processes.

Collisional redistribution amongst the excited states of the beam atoms is primarily due to electron and ion impact excitation from the He($1s^2 \ ^1S$) ground and

neighbouring excited states. In the plasma, these processes are also accompanied by their corresponding reverse reactions. That is electron and ion impact de-excitation. Electrons can populate both the singlet and triplet excited states whilst ions can only populate the excited singlet states. This is due to the fact that for a spin changing transition to occur an exchange reaction between like particles is required. We show in figure 2.6 the behaviour of electron and ion (D^+) impact excitation from the $He(1s^2\ ^1S)$ ground state to various excited singlet levels.

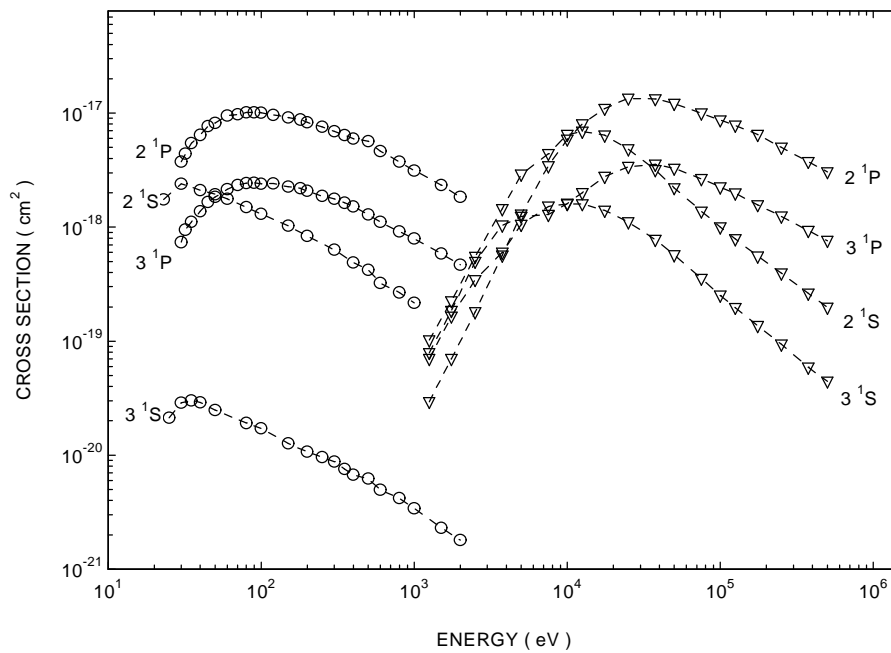


Figure 2.6 Cross sections for electron and ion impact excitation from the $He(1s^2\ ^1S)$ ground state to various excited singlet levels . O : Electron impact excitation, ∇ : Ion (D^+) impact excitation .

Electron impact excitation, as mentioned before, can also contribute to populating the triplet excited levels. This can occur through direct excitation from the ground state of the beam atoms or via excited state transitions from the singlet to triplet spin system. In figure 2.7 we show the behaviour of electron impact excitation from the ground to various excited triplet states. Also shown is the electron impact excitation cross sections from the $He(2s\ ^3S)$ metastable level to neighbouring excited levels.

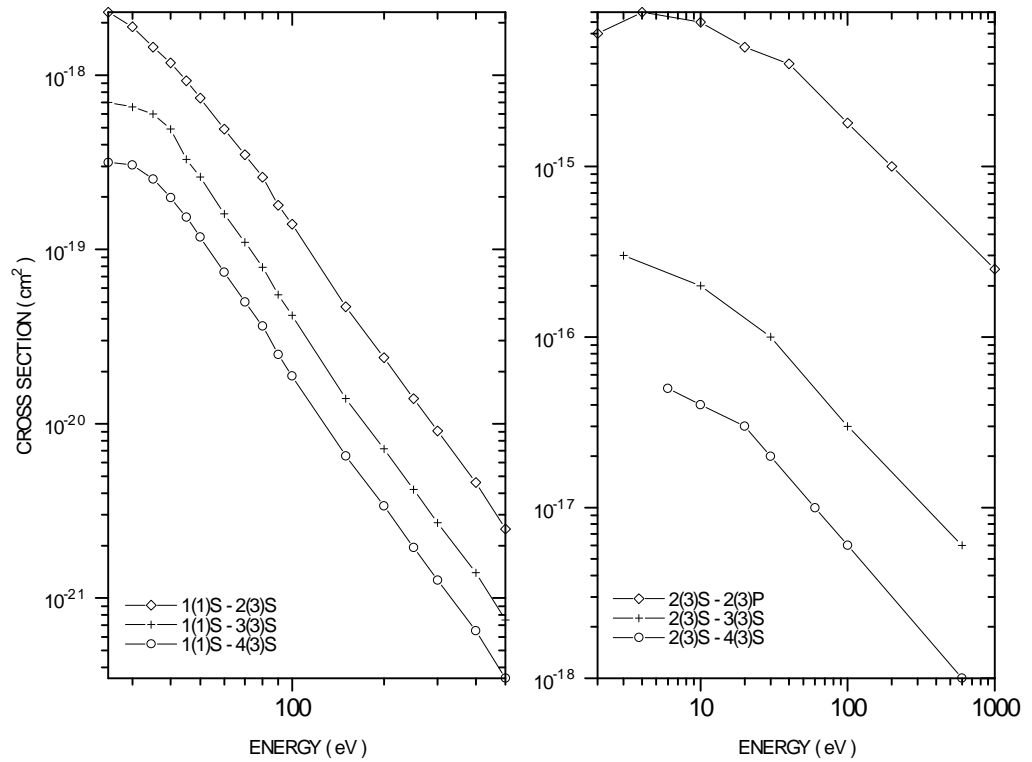


Figure 2.7 Cross sections for electron impact excitation. The figure to the left illustrates the behaviour of excitation from He($1s^2\ ^1S$) to excited triplet levels. The figure to the right contains excitation cross sections for transitions from the He($2s\ ^3S$) metastable to neighbouring excited levels.

Due to the presence of metastable levels in helium i.e. He($2s\ ^1S$) and He($2s\ ^3S$), we should also focus our attention on the atomic processes associated with these levels. The motivation being that the metastable population may become significant as the beam penetrates into the plasma. Therefore the associated atomic processes will contribute substantially to stripping the electrons from the beam atoms. In figure 2.8 we show the behaviour of the primary atomic processes which contribute to stripping the electrons from the He($2s\ ^3S$) metastable level.

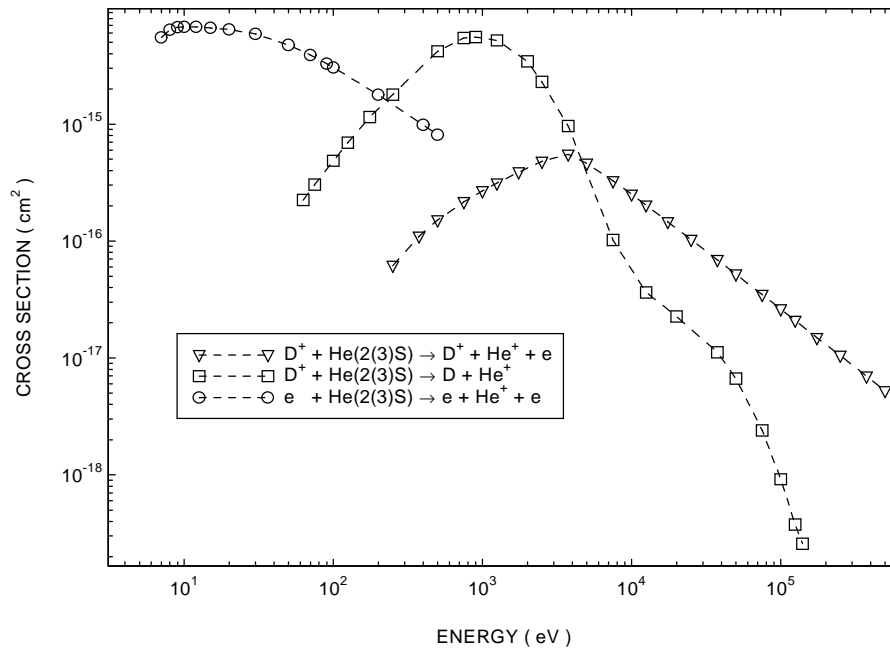


Figure 2.8 Cross sections for the atomic processes which contribute to stripping the electrons from the He($2s^3S$) metastable level.

As can be seen, electron impact ionisation dominates until ~ 200 eV where the contribution due to charge exchange becomes substantial. In the usual manner ion impact ionisation competes with charge exchange. It is of interest to compare the behaviour of the atomic processes shown in figure 2.8 with the corresponding processes associated with the He($1s^2^1S$) ground state, see figure 2.5. The cross sections involving the He($2s^3S$) level are larger than that associated with the ground state. It can also be observed that the charge exchange cross section associated with the triplet metastable begins to dominate at ~ 200 eV and continues to do so until ~ 5.0 keV. In the case of the ground state the dominant behaviour of the charge exchange process occurs from ~ 750 eV to ~ 17.5 keV.

The influence of impurities contained in the plasma should also be taken into consideration since they will contribute to stripping the electrons from the helium beam atoms. In figure 2.9 we illustrate the behaviour of single and double charge exchange associated with the ground state of the beam atoms for a selected range of fully stripped ions which are common plasma impurities.

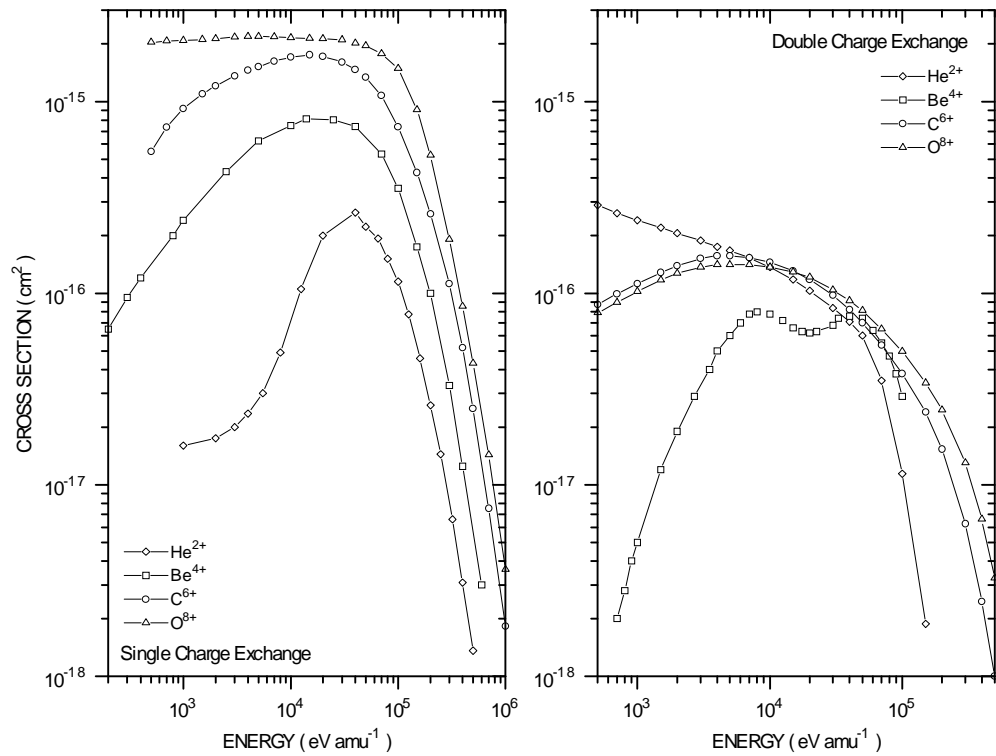


Figure 2.9 Single and double charge exchange cross sections associated with the $\text{He}(1s^2 \ ^1S)$ ground state. The figure to the left illustrates the cross sections for single charge exchange for a selected range of fully stripped ions which are common plasma impurities. The figure to the right shows the cross sections for double charge exchange.

As illustrated in the figure above, single charge exchange exceeds double charge exchange for all the ions with the exception of fully stripped helium. Below $\sim 10 \text{ keV amu}^{-1}$ double charge exchange dominates single charge exchange for helium. Double charge exchange between fully stripped helium and neutral helium atoms is a symmetrical resonant process and as a consequence has a large cross section[31]. In figure 2.10, we illustrate the behaviour of single and double ion impact ionisation for a similar variety of fully stripped plasma impurity ions.

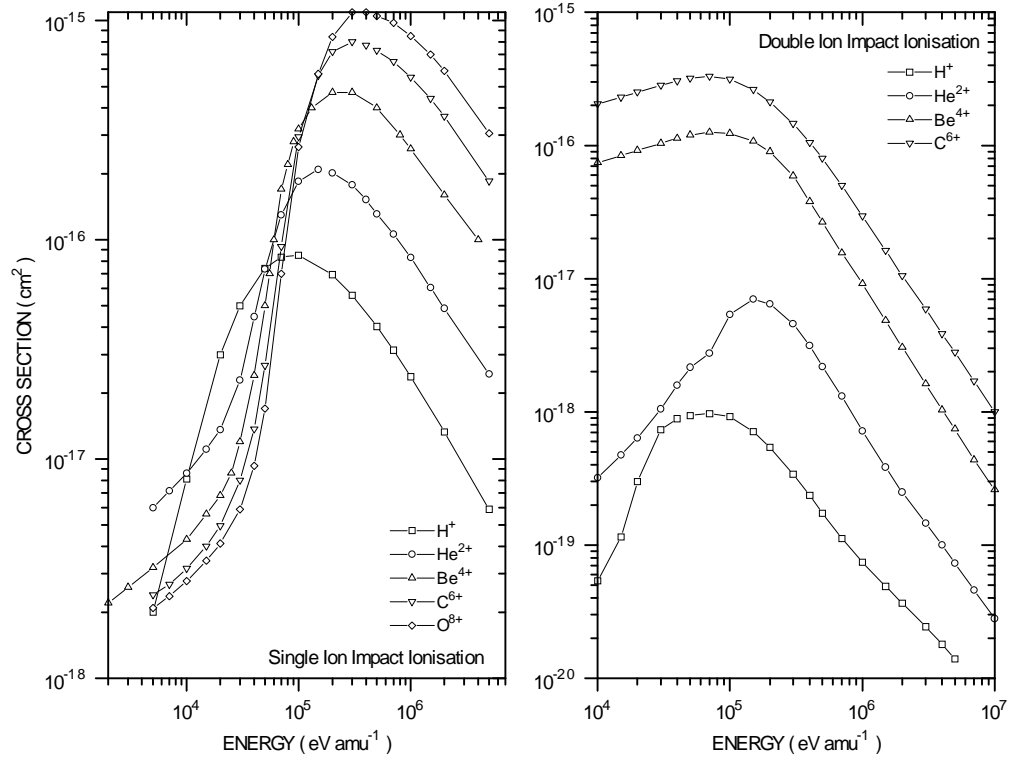


Figure 2.10 Cross sections for single and double ion impact ionisation from the $\text{He}(1s^2 \ ^1S)$ ground state of the beam atoms. The figure to the left shows the cross sections for single ion impact ionisation for a variety of fully stripped ions which are common plasma impurities. Also shown in the figure for comparison is the cross section describing single ion impact ionisation due to H^+ . The figure to the right illustrate the cross sections for double ion impact ionisation for a similar range of plasma impurities.

We must also take into consideration the contribution due to the plasma impurity ions at stripping electrons from the metastable levels of the beam atoms. In figure 2.11 we show the cross sections for charge exchange and ion impact ionisation from the $\text{He}(2s \ ^3S)$ metastable for a selected range of fully stripped plasma impurities.

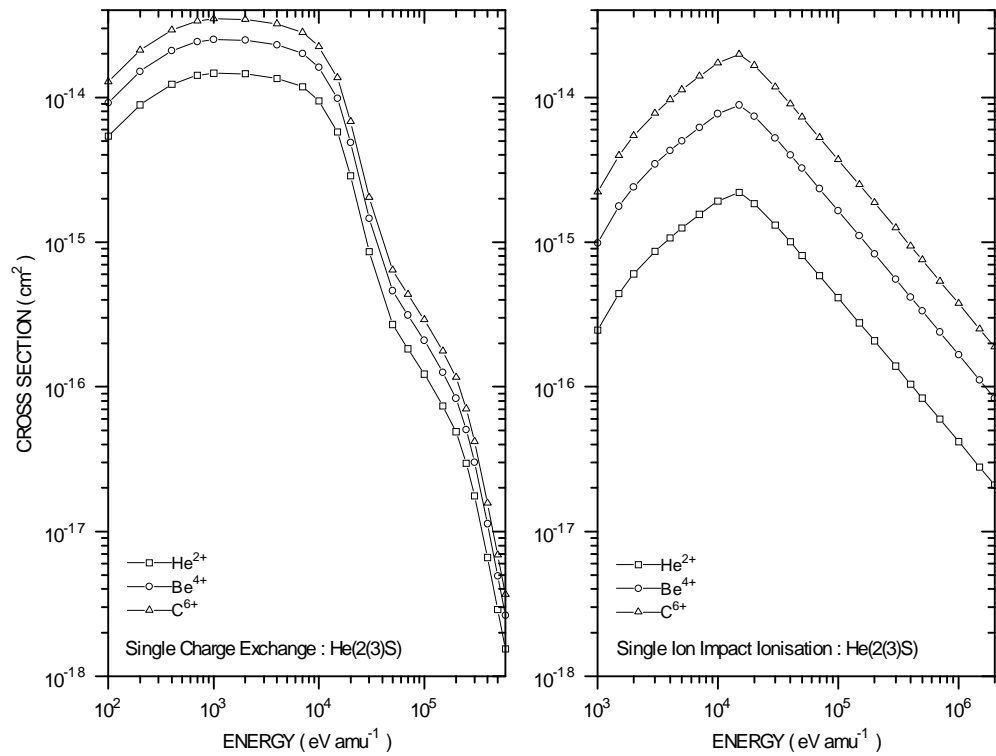


Figure 2.11 Charge exchange and ion impact ionisation from He($2s\ ^3S$) metastable level. The figure to the left illustrates the cross sections for single charge exchange for various fully stripped plasma impurity ions. The figure to the right exhibits the cross sections for ion impact ionisation.

It is of interest to compare the charge exchange cross sections shown above with the cross sections associated with the ground state of the beam atoms, see figure 2.9. It can be observed that the cross sections associated with the He($2s\ ^3S$) level are substantially larger than the cross sections associated with the ground state.

2.5 Approaches to modelling

When fast neutral beam atoms are injected into a tokamak plasma, the impurity ion impact atomic processes which excite and ionise the beam neutrals are the most important and so the population structure is primarily governed by the ion density. There are three different ‘pictures’ of the population structure which apply to the particular regimes of the ion density. These are schematically shown in figure 2.12

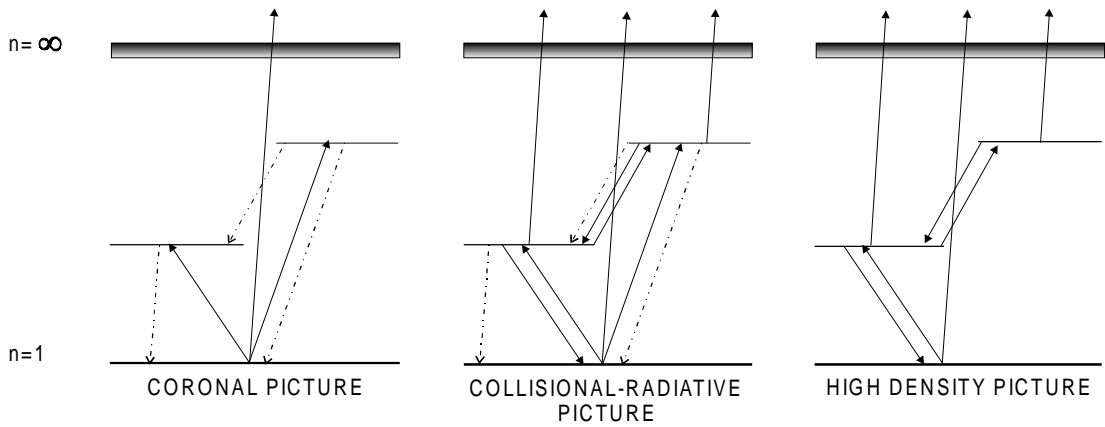


Figure 2.12 Schematic energy level structure of an arbitrary beam atom. The dashed and solid lines represent the radiative and collisional processes respectively. Working from left to right. Firstly the coronal picture, the beam atoms can only be ionised by direct collisional ionisation from the ground state. Next is the collisional-radiative picture where the beam atoms can be ionised by direct and stepwise atomic processes. Finally, the high density picture which describes the regime where the collisional processes completely dominate the radiative processes. Ionisation is due to direct and stepwise collisional processes, excitation also contributes to ionisation.

The first ‘picture’ applies to a low density plasma ($< 1.0 \times 10^{11} \text{ cm}^{-3}$ for pure D^+ plasma) where the conditions are such that the beam atoms can only be ionised by collisional ionisation (which may include charge transfer) from their ground state. There is no significant contribution to ionisation from the excited states. This is due to the fact that in this regime the excited populations are low relative to the ground population. The excited levels are populated by electron and ion impact excitation from the ground but rapidly depopulate by radiative decay before any further excitation or ionisation can occur. This is described as the coronal picture.

As the ion density of the plasma increases ($\sim 1.0 \times 10^{13} \text{ cm}^{-3}$ for a pure D^+ plasma), the influence of the collisional processes increases so that a competition with the radiative processes commences. The beam atom population structure is now determined by a wide range of collisional and radiative processes associated with their ground and excited states. The beam neutrals can now be ionised by direct and stepwise atomic processes. This is called the collisional-radiative picture.

The last ‘picture’ which is of interest occurs when the ion density of the plasma is increased substantially ($\sim 1.0 \times 10^{18} \text{ cm}^{-3}$ for a pure D^+ plasma), so that

collisional processes completely dominate the radiative processes. The contribution to the ionisation of the beam atoms is due to direct and stepwise collisional atomic processes associated with the ground and excited states. The excited state populations diminish. This is called the high density picture. In such a regime the condition of local thermodynamic equilibrium is achieved both for high and low lying levels.

2.5.1 Coronal equilibrium model

The coronal picture gives the simplest approach to obtain the excited state population structure of the beam atoms, as well as the rate at which they are being ionised. In this case, for the ionisation loss from the ground state there is no need to consider the contribution from the excited states. If we consider a simple case where the beam atoms have no metastables and the plasma is free of impurities, the statistical balance equations for the excited levels ($i > 1$) are of the form,

$$v_b \frac{dN_i}{dx} = \left(N_1 n_e q_{1 \rightarrow i}^e + N_1 n_p q_{1 \rightarrow i}^p + \sum_{j>i} N_j A_{j \rightarrow i} \right) - \left(\sum_{j<i} N_i A_{i \rightarrow j} \right) \quad 2.14$$

for $i = 2, 3, \dots$

where N_1 corresponds to the population of the ground state, $q_{1 \rightarrow i}^e$ and $q_{1 \rightarrow i}^p$ are the collisional excitation rates to level i due to electrons and protons respectively. The quantity $A_{i \rightarrow j}$ is the transition probability from the level i to level j . The population structure can be obtained by assuming the excited levels have relaxed and reached equilibrium relative to the instantaneous ground population. Therefore $v_b dN_i/dx = 0$ and equation 2.14 reduces to a set of linear equations which yield the excited populations relative to the ground state population N_1 by downward recursion. The corresponding statistical balance equation for the ground state is given as,

$$v_b \frac{dN_1}{dx} = \left[\sum_{j>1} N_j A_{j \rightarrow 1} \right] - \left[\sum_{j>1} (n_e q_{1 \rightarrow j}^e + n_p q_{1 \rightarrow j}^p) N_1 + (n_e q_{1 \rightarrow \infty}^e + n_p q_{1 \rightarrow \infty}^p + n_p q_{1 \rightarrow \infty}^{CX}) N_1 \right] \quad 2.15$$

where $q_{1 \rightarrow \infty}^e$, $q_{1 \rightarrow \infty}^p$ and $q_{1 \rightarrow \infty}^{cx}$ are the respective contributions due to direct electron and proton impact ionisation as well as charge exchange. If we then substitute equation 2.14, under the assumption that the excited states have reached equilibrium, into equation 2.15 we arrive at,

$$v_b \frac{dN_1}{dx} = -\left(n_e q_{1 \rightarrow \infty}^e + n_p q_{1 \rightarrow \infty}^p + n_p q_{1 \rightarrow \infty}^{cx}\right) N_1 \quad 2.16$$

Assuming that the majority of the beam atoms are initially in their ground state, this equation can then be used to model the attenuation of the beam. It is more convenient though to describe the attenuation of the beam in terms of an effective stopping cross section which is defined as,

$$\sigma_s = \left[q_{1 \rightarrow \infty}^e + \frac{n_p}{n_e} \left(q_{1 \rightarrow \infty}^p + q_{1 \rightarrow \infty}^{cx} \right) \right] \frac{1}{v_b} \quad 2.17$$

where σ_s is the effective beam stopping coefficient. The effective stopping coefficient can then be used to evaluate the beam attenuation at any given point along the beam using the following relation,

$$n_b = n_0 \exp\left(- \int n_e \sigma_s dl\right) \quad 2.18$$

where n_0 is the initial beam density on entry to the plasma and dl is along the path taken by the neutral beam. It should be noted however that equation 2.18 is only valid provided the beam atoms of interest does not contain any long lived metastable levels.

2.5.2 Collisional-radiative model

The simple coronal picture however is only applicable for low density plasmas where the radiative processes occur on time scales faster than the collisional processes. In tokamak plasmas the ion densities are sufficiently high and encourage the collisional

processes to compete with the radiative processes. The excited states of the beam atoms are populated and depopulated by both collisional and radiative processes. This is the so called collisional-radiative picture. The statistical balance equations for an arbitrary beam atom are,

$$\begin{aligned}
v_b \frac{dN_i}{dx} = & \sum_{i' > i} (A_{i' \rightarrow i} + n_e q_{i' \rightarrow i}^e + n_p q_{i' \rightarrow i}^p) N_{i'} + \sum_{i'' < i} (n_e q_{i'' \rightarrow i}^e + n_p q_{i'' \rightarrow i}^p) N_{i''} + \\
& \left(\alpha_i^{RR} + \alpha_i^{DR} + \frac{n_b}{n_e} \alpha_i^{CX} + \alpha_i^{(3)} n_e \right) n_+ n_e - \sum_{i' < i} (A_{i \rightarrow i'} + n_e q_{i \rightarrow i'}^e + n_p q_{i \rightarrow i'}^p) N_{i'} \\
& - \sum_{i' > i} (n_e q_{i \rightarrow i'}^e + n_p q_{i \rightarrow i'}^p) N_{i'} - (n_e q_{i \rightarrow \infty}^e + n_p q_{i \rightarrow \infty}^p + n_p q_{i \rightarrow \infty}^{CX}) N_i
\end{aligned} \quad 2.19$$

for $i = 1, 2, 3, \dots$

where $i'' < i < i'$ and $q_{i \rightarrow i'}$ is the excitation rate from state i to i' by electrons and protons according to the superscript. The corresponding de-excitation rate is given as $q_{i' \rightarrow i}$ and $A_{i' \rightarrow i}$ is the spontaneous emission coefficient for the radiative transition from level i' to i . Impact ionisation is represented by $q_{i \rightarrow \infty}$ where the superscript indicates whether it is by electrons or protons and the rate coefficient for charge exchange from state i is given as $q_{i \rightarrow \infty}^{CX}$. The quantities α^{RR} , α^{DR} and $\alpha^{(3)}$ are respectively the contributions due to radiative, dielectronic and three-body recombination. The quantity α^{CX} is the contribution due to charge exchange where the beam atoms themselves are the donors. It should be noted though that since the beam atoms are in a strictly ionising environment the latter and former recombining processes only become of interest when the neutral beam atoms are moving with such a slow velocity that they can be considered stationary. In which case the statistical balance equations describe the conditions of a thermal plasma rather than a point in the plasma which is traversed by a neutral beam.

The statistical balance equations in equation 2.19 form the basis of what is formally known as collisional-radiative modelling and is the method adopted in this work. Collisional-radiative modelling, as originally developed by Bates et. al.[32], involves solving the statistical balance equations while taking into consideration the influence of stepwise atomic processes. Quantities such as the excited population

structure and collisional-radiative coefficients are of interest. The collisional-radiative coefficients include effective cross coupling, ionisation and recombination coefficients.

To recast the statistical balance equations into the framework of generalised collisional-radiative theory a common starting point is to write equation 2.19 using matrix notation,

$$v_b \frac{dN_i}{dx} = n_e n_+ r_i - \sum_j C_{ij} N_j \quad 2.20$$

for $i = 1, 2, 3, \dots$

where C_{ij} ($C_{ij} \equiv C_{j \rightarrow i}$) is the collisional-radiative matrix for which the matrix elements are defined as follows.

$$C_{ij} = \begin{cases} A_{j \rightarrow i} + n_e q_{j \rightarrow i}^e + n_p q_{j \rightarrow i}^p & j > i \\ n_e q_{j \rightarrow i}^e + n_p q_{j \rightarrow i}^p & j < i \end{cases} \quad 2.21$$

and,

$$C_{ii} = - \sum_{j < i} \left(A_{i \rightarrow j} + n_e q_{i \rightarrow j}^e + n_p q_{i \rightarrow j}^p \right) - \sum_{j > i} \left(n_e q_{i \rightarrow j}^e + n_p q_{i \rightarrow j}^p \right) - n_e q_{i \rightarrow \infty}^e - n_p q_{i \rightarrow \infty}^p - n_p q_{i \rightarrow \infty}^{CX} \quad 2.22$$

The variable r_i is the composite recombination coefficient and is defined as,

$$r_i = \alpha_i^{RR} + \alpha_i^{DR} + \frac{n_b}{n_e} \alpha_i^{CX} + \alpha_i^{(3)} n_e \quad 2.23$$

Following the work of Spence[19], if we generalise and assume that the beam atoms of interest have m ‘non-equilibrium’ levels (that is levels whose populations are not locally relaxed), we can separate the ordinary excited levels which have reached local equilibrium from the non-equilibrium levels. Letting N_j^{eq} denote the equilibrium excited level populations then,

$$v_b \frac{dN_\rho}{dx} = n_e n_+ r_\rho - \sum_j C_{\rho j} N_j \quad 1 \leq \rho \leq m \quad 2.24$$

$$v_b \frac{dN_i}{dx} = 0 = n_e n_+ r_i - \sum_j C_{ij} N_j^{eq} \quad i > m \quad 2.25$$

where equation 2.24 describes the population of the non-equilibrium levels which are denoted by the Greek subscript ρ . The ground state is of course such a non-equilibrium level. Generally the ground state and metastable states are the non-equilibrium levels for beams in fusion plasmas. Equation 2.25 describes the behaviour of the excited levels which have reached equilibrium. Separating the non-equilibrium and equilibrium populations in 2.24 and 2.25 gives,

$$v_b \frac{dN_\rho}{dx} = n_e n_+ r_\rho - \sum_{j>m} C_{\rho j} N_j^{eq} - \sum_{\sigma=1}^m C_{\rho\sigma} N_\sigma \quad 2.26$$

$$0 = n_e n_+ r_i - \sum_{j>m} C_{ij} N_j^{eq} - \sum_{\sigma=1}^m C_{i\sigma} N_\sigma \quad 2.27$$

Therefore the equilibrium population can be obtained by multiplying equation 2.27 by the inverse of C_{ij} ,

$$N_j^{eq} = n_e n_+ \sum_{i>m} C_{ji}^{-1} r_i - \sum_{i>m} \sum_{\sigma=1}^m C_{ji}^{-1} C_{i\sigma} N_\sigma \quad j > m \quad 2.28$$

If we now substitute this equation back into equation 2.26 we arrive at,

$$v_b \frac{dN_\rho}{dx} = n_e n_+ \left[r_\rho - \sum_{j>m} \sum_{i>m} C_{\rho j} C_{ji}^{-1} r_i \right] - \sum_{\sigma=1}^m \left[C_{\rho\sigma} - \sum_{j>m} \sum_{i>m} C_{\rho j} C_{ji}^{-1} C_{i\sigma} \right] N_\sigma \quad 2.29$$

Which is more commonly written in terms of the time derivative as,

$$\frac{dN_\rho}{dt} = n_e n_+ \alpha_\rho - n_e \sum_{\sigma=1}^m S_{\rho\sigma} N_\sigma \quad 2.30$$

where $S_{\rho\sigma}$ is the cross coupling coefficient for the non-diagonal elements while the diagonal elements include the effective ionisation coefficient,

$$S_{\rho\sigma} = \left(C_{\rho\sigma} - \sum_{j>m} \sum_{i>m} C_{\rho j} C_{ji}^{-1} C_{i\sigma} \right) \frac{1}{n_e} \quad 2.31$$

and α_ρ is the collisional-radiative recombination coefficient,

$$\alpha_\rho = r_\rho - \sum_{j>m} \sum_{i>m} C_{\rho j} C_{ji}^{-1} r_i \quad 2.32$$

The rate at which electrons recombine from the continuum onto a non-equilibrium level ρ is given by the recombination coefficient α_ρ . The cross coupling coefficients describe the rate at which the non-equilibrium levels, including the ground state, are populated and depopulated within a collisional-radiative frame work. The cross coupling coefficients can also be used to obtained the collisional-radiative ionisation coefficients. These coefficients represent the rate at which the non-equilibrium levels of the beam atoms are ionised and are obtained using the following expression,

$$S_\rho = S_{\rho\rho} - \sum_{\sigma=1}^{\rho-1} S_{\rho\sigma} - \sum_{\sigma=\rho+1}^m S_{\rho\sigma} \quad 2.33$$

In the case of a deuterium beam, the only non-equilibrium level is the ground state. The $2s \ ^2S$ level is not a non-equilibrium level since there is strong $2s \ ^2S \rightarrow 2p \ ^2P$ collisional and field mixing. There are no cross coupling coefficients, only the single collisional-radiative ionisation coefficient. On the assumption that only the ground state of the beam atoms is significantly populated, this coefficient can be used to describe the rate at which the beam atoms are ionised and is commonly referred to as the effective beam stopping coefficient. It is converted into an effective beam stopping cross section by dividing through with the beam velocity. Using equation 2.18 the attenuation of a neutral deuterium beam can be calculated. The equilibrium populations of the excited states are simply evaluated relative to the ground state are equation 2.28.

For a neutral helium beam, there are three non-equilibrium levels. The ground state and the two metastable levels ($\text{He}(2 \ ^1S)$ and $\text{He}(2 \ ^3S)$). There is a total of nine

cross coupling coefficients and three effective ionisation coefficients. The Greek subscripts of equation 2.31 indicate the initial and final states associated with each coefficient. The diagonal elements represent the total population loss rate from the specified non-equilibrium level. This total loss rate includes the loss rate to the continuum as well as to the other remaining non-equilibrium levels, whilst the effective ionisation coefficients describe the rate at which electrons are lost from each of the non-equilibrium levels to the continuum. To model the attenuation of the beam we can no longer employ the simple expression of equation 2.18, a spatially dependent solution of the following set of equations is required.

$$\begin{aligned}
v_b \frac{dN_{1^1S}}{dx} &= n_e S_{1^1S} N_{1^1S} - n_e S_{2^1S \rightarrow 1^1S} N_{2^1S} - n_e S_{2^3S \rightarrow 1^1S} N_{2^3S} \\
v_b \frac{dN_{2^1S}}{dx} &= -n_e S_{1^1S \rightarrow 2^1S} N_{1^1S} + n_e S_{2^1S} N_{2^1S} - n_e S_{2^3S \rightarrow 2^1S} N_{2^3S} \\
v_b \frac{dN_{2^3S}}{dx} &= -n_e S_{1^1S \rightarrow 2^3S} N_{1^1S} - n_e S_{2^1S \rightarrow 2^3S} N_{2^1S} + n_e S_{2^3S} N_{2^3S}
\end{aligned} \tag{2.34}$$

where $N_{n \ 2S+1 \ L}$ is the population of the level specified by the quantum numbers n , S and L . The contribution to the equilibrium population of each excited state from each non-equilibrium level is calculated using equation 2.28.

2.6 Previous theoretical studies

2.6.1 Modelling neutral deuterium beam

The first attempt at modelling the attenuation of a neutral deuterium beam, as it entered into a tokamak plasma, was reported by Riviere[33] in 1971. Riviere employed a simple coronal type model to investigate the penetration depth of a beam as a function of typical plasma parameters. The approach of using a simple coronal type model was continued by many others[21, 34], even after the work of Boley et. al.[35]. Boley et. al. demonstrated that a collisional-radiative description was necessary to include all the atomic processes which contribute to ionising the beam

neutrals. A series of coupled differential equations, which spanned from the ground state to the Lorentz ionisation limit associated with the beam atoms, was employed to model the effective ionisation of the beam neutrals and hence the beam attenuation.

Although a lot of information regarding the beam attenuation was now available, little was known about the behaviour of the excited state population structure until the work of Summers[36] and the later efforts of Spence[19] at JET Joint Undertaking. Using a code which was originally based on the earlier work of Burgess and Summers[37], a detailed description of the excited population structure of the beam atoms was now readily available. Interest in the excited population structure of the beam atoms grew and was later modelled by Korotkov[38]. Using the method described by Boley et. al., Korotkov investigated both the excited population structure and the attenuation of neutral deuterium beam atoms. The excited state populations were calculated in what we describe as the bundled-n approximation. In which the population of each principal quantum shell are evaluated.

Due to the increased availability of high quality atomic data, the attenuation calculations of Korotkov were later revised by Janev et. al[39]. Janev et. al. conducted a more elaborate study of the beam attenuation and presented analytical fits to the effective beam stopping cross sections.

The present work develops from the original JET collisional-radiative model where we assemble a series of statistical balance equations in the bundled-nS approximation. The method of solution is complete and enables one to conduct a detailed study of the effective stopping coefficients as well as the excited state population structure. The code systematically accesses the most recent fundamental atomic data and employs a wide variety of formulae to generate the cross sections for transitions where there is no fundamental data available. We do not present our data in terms of analytical fits. ADAS as a matter of policy archives exact numerical data. The analytical fits of Janev et. al. are unsound in the low and high density asymptotic limits of the effective beam stopping cross sections. As an example we show in figure 2.13, a comparison between the results obtained in this work and the analytical fits of Janev et. al. as a function of beam energy

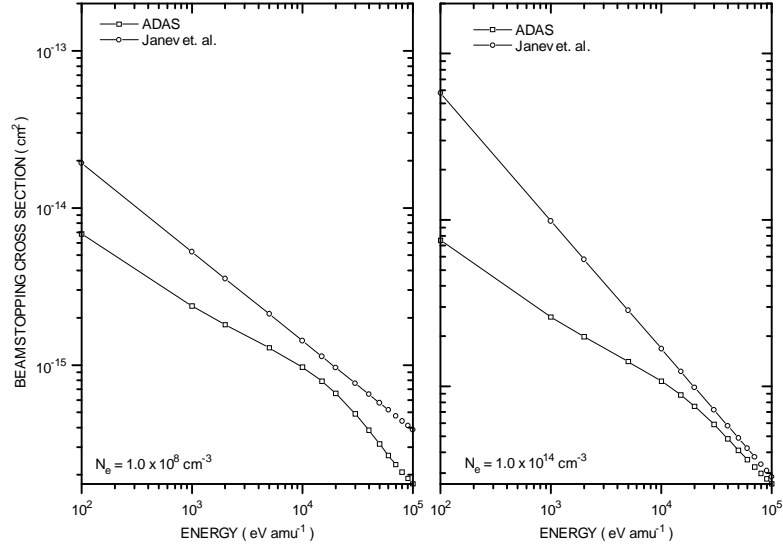


Figure 2.13 Beam stopping cross sections Vs energy for a pure H^+ plasma. Comparison between the analytical fits of Janev et. al.[39] and the results obtained from this work. The densities where selected to illustrate the difference at the coronal limit ($1.0 \times 10^8 \text{ cm}^{-3}$) and near the high density regime ($1.0 \times 10^{14} \text{ cm}^{-3}$).

2.6.2 Modelling a neutral helium beam

The application of a neutral helium beam as an edge or as a core diagnostic needs slightly different modelling approaches. As an edge diagnostic, a slow beam is employed to penetrate into the periphery of the plasma where the conditions are usually such that a spatially dependent solution of the statistical balance equations is required[12, 13]. For a fast neutral helium beam as a core diagnostic, the excited levels, with the exception of the metastables, have reached local equilibrium. There had been various attempts to model the attenuation and excited population structure of fast neutral helium beams[38,40]. However, the most significant contribution was due to the later work of Korotkov[41]. Using a series of coupled equations, Korotkov investigated the behaviour of the excited population structure and the beam attenuation under the assumption that the metastable levels had relaxed and reached equilibrium. The excited populations were calculated in what we describe as the bundled-nlSL approximation. The bundled-nlSL approximation involves evaluating

the population for each of the angular sub-states for the low lying levels, while the population of the higher levels are calculated in a bundled-nS approximation.

An attempt to include the influence of the non-equilibrium metastable levels on the population structure and attenuation was undertaken by a combined effort of Korotkov and Janev[42]. In addition to using improved fundamental data, Korotkov et. al., introduced an approximate method to describe the influence of the non-equilibrium levels.

In this work we model the attenuation and population structure of a neutral helium beam by assembling the complete set of coupled equations in the bundled-nSL approximation. The method of solution here however is more general and complete since we do not assume that the metastable level populations have relaxed. In these circumstances, the attenuation of the beam is no longer characterised by a single stopping coefficient. Rather it is described by a coupled set of three equations linked by collisional-radiative cross coupling coefficients. These cross coupling coefficients are also calculated in the full bundled-nSL model. We give considerable attention to using the most recent fundamental data and as for deuterium employ a variety of approximate methods to generate cross sections for transitions where there is no fundamental data available.